ISSN 2712-0554
Original Research

Heritage and Sustainable Development
Vol. 6, No. 1, March 2024, pp.183-196
https://doi.org/10.37868/hsd.v6i1.306

Solar desalination with charcoal briquettes from plants as an additional absorption sorbent

Muhamad Jafri[1*], Ben Vasco Tarigan[1], Dominggus Godlief Heryson Adoe[1]
[1] Department of Mechanical Engineering, Faculty of Sciences and Engineering, Universitas Nusa Cendana, Kupang, Indonesia

*Corresponding author E-mail: muhamad_jafri@jstaf.undana.ac.id

Received Nov. 21, 2023
Revised Mar. 15, 2024
Accepted Mar. 19, 2024

Abstract

Water is the most abundant substance on Earth, but only 2.5% can be used for drinking and farming; the rest is seawater containing much salt. Solar desalination is a great tool to solve this problem for small families and remote areas. However, the disadvantage of using solar power is still the low productivity of distillate because it depends on the season, region, and intensity of solar radiation. Solar radiation heat absorbing and storing materials are a favorable solution in increasing evaporation rate, efficiency, and total distillate. Many have been developed to date, but these materials require more expenditure to be used as radiation heat sinks and stores. Charcoal derived from wood has high thermal energy absorption and porosity. Four desalination devices were used, namely using an additional absorber made from Kapok wood (Ceiba pentandra) coded CP_60, Gamal wood (Gliricidia sepium) coded GS_60, Kusambi wood (Schleichera oleosa) coded SO_60, and without additional absorber as a comparison. All desalination devices have the same shape and size, simple, with an area of 0.09 m^2 each. Before the additional absorber base material is used, drying, charring, grinding, meshing, pressing, and briquetting are carried out. The test results show that the additional absorber of natural materials affects the evaporation rate, desalination efficiency, and total distillate water. The distillation device using Gamal wood (Gliricidia sepium) additional absorber material, coded GS_60, provides maximum performance such as distillate water yield every 30 minutes and total distillate 124 ml/0.09 m^2, 28.19% efficiency, and evaporation rate.

Keywords: Desalination, Solar still, Natural absorption, Charcoal briquettes

1. Introduction

The most abundant substance on Earth is water, but only 2.5%, because the rest is seawater, which contains high salt elements [1]. Desalination technology is an exciting option to provide clean water [2]. The technologies are highly developed, such as multi-stage flash evaporation (MSF), multi-effect distillation (MED), vapor compression (VP), reverse osmosis (RO), forward osmosis (FO), and electrodialysis/electrodialysis reversal (ED/EDR) [3]. However, these technologies require conventional energy sources such as fossil fuels or electricity [4]. Fossil fuel desalination is estimated to contribute 400 million tonnes per year of global emissions over the last 25 years. Renewable energy use for the desalination process, such as solar thermal energy, is necessary [5][6]. Therefore, the desalination process is challenging to implement in remote areas due to its high cost and unavailability of conventional energy.

Solar energy is a widely used renewable energy source because it is environmentally friendly, has easy availability, and the radiation flux reaching the Earth is about 8 × 104TW [7]. There are two types of desalination techniques developed that utilize solar energy effectively, namely solar photovoltaics and solar thermal collectors [8]. In the desalination process, solar energy is used to heat and raise the temperature of seawater to increase the evaporation rate [9]. Solar thermal energy utilization for industry and households as drying, space heating, water heating, and seawater desalination, through solar panels has been tested [10]. However, the disadvantage of solar energy desalination is still the low productivity of the distillate because it is highly dependent on the season, region, and intensity of irradiation in a day [11]. Other researchers claim two reasons for the low productivity of solar-powered desalination. Firstly, it is difficult to release the latent heat of condensation into the atmosphere and secondly, it is difficult to increase the evaporation temperature and reduce the condensation temperature [12].

Due to the above limitations, several innovative techniques have been investigated, such as externally cooled thermoelectric modules [13], parabolic dish concentrators [13][14], mirrors [15][16], porous media [17], ultrasonic humidification materials [18], heat pipes [19], external condensers [20], energy storage [21], and nanoparticles [22]. In addition to the above parameters, heat storage materials are a promising solution in improving solar stills' heat and mass transfer. Such materials provide higher surface area [23], such as gravel [24][25], metal wire sponge [26], and many more to increase the water temperature in the solar desalination basin. However, these materials require more energy for radiation heat absorbers and storage. So, it is necessary to develop radiation heat absorbing and storing cheap, easy-to-obtain, and abundant materials.

Charcoal derived from wood has high thermal energy absorption and porosity. How charcoal is used in various forms significantly influences freshwater productivity. Using charcoal creates a larger surface for radiation and convective heat transfer [27]. Adding charcoal to water increases the energy supply for evaporation by increasing the absorption of solar energy into the water, and is a good material for absorbers/evaporators and water transport media [28][29].

These charcoal materials store 5-14 times more heat per unit volume than water-sensible storage materials. Also, economic considerations and availability are abundant [30]. The use of charcoal to improve evaporation efficiency in the desalination process has been carried out [31][29], using charcoal blocks can increase repair by 8% [32], and charcoal in use can increase productivity by 15% compared to wick type still, and it also has the advantage of low thermal capacity [23]. Many energy-absorbing and storing organic, inorganic, and eutectic materials are available based on the required temperature range. However, we must use the available materials and cover the poor physical properties with adequate system design. Kapok wood (Ceiba pentandra), Gamal wood (Gliricidia sepium), and Kusambi wood (Schleichera oleosa) are abundant in the world. The purpose of this research is to increase the evaporation rate, desalination efficiency, and volume of desalinated water by utilizing the potential of natural materials of kapok charcoal briquettes (Ceiba pentandra), Gamal (Gliricidiasepium), and Kusambi (Schleichera oleosa), to absorb solar energy.

2. Research method

2.1. Description and operating principle

The desalination test media used four basins with the model of Figure 1, the same as that developed by [33], where the shape of the basin is a combination of a pyramid and a cuboid. The basin walls are made of 9 mm plywood on the outside and 2 mm acrylic painted black on the inside. The cuboid of the basin has a 30 cm length, 30 cm width, and 10 cm height. The pyramid section has a 30 cm length, and 30 cm width, and the height of the back of the pyramid is 20 cm. This size considers the length of the path traveled by the distillate water from the top of the cover through the distillate channel. Basin has two stages which are made from isolator material multiplexes that have a thick 12 mm. The inside of the basin was made from acrylic with 2 mm thickness. The color of the inside basin is black which functions as a heat absorber of solar thermal. The cover of the basin uses 2 mm transparent glass. This cover is a part where condensations occur. The top side is made of 2 mm transparent glass as the basin cover with a 30° orientation to the horizontal with dimensions of 30 cm x 30 cm. Glass selection refers to the previous research on glass thickness [34] [35] and the angle of the glass to the horizontal plane of 30° [36]. In the bottom of the basin, a plastic pipe with a diameter of 0.4 cm was installed to channel the distillate water to the container outside.

The absorbent plate and additional absorbent in wood-based charcoal briquettes in the basin with seawater absorb solar radiation heat. Charcoal briquettes not only have heat-absorbing characteristics but also have good heat energy storage properties. Because of the heat stored in the charcoal briquettes and the characteristics of seawater, namely wetness and capillarity when in contact with charcoal briquettes (solid objects), seawater rises faster to the surface of the charcoal briquettes and eventually evaporates. The water vapor migrates upwards to the glass cover of the basin.

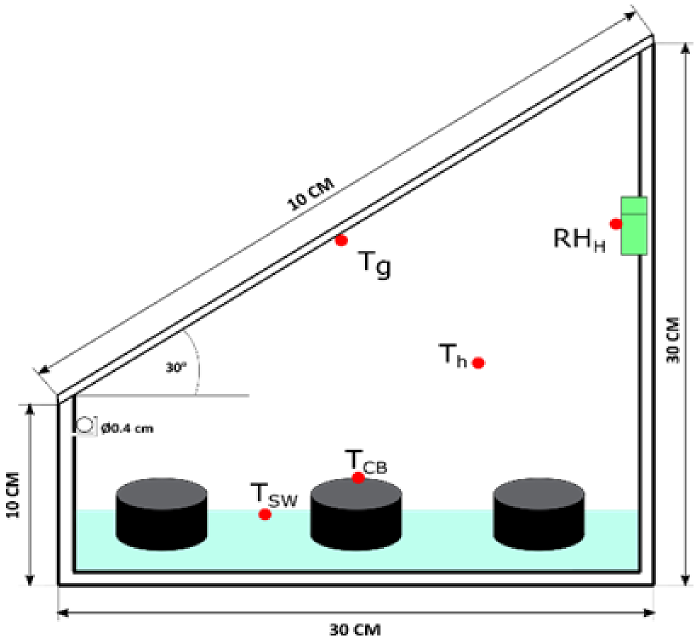

T_g = glass temperature, RH_H = room humidity, T_h = basin room temperature, T_{CB} = surface temperature of charcoal briquettes and T_{sw} = water surface temperature.

Figure 1. Design of test equipment

The glass temperature is much lower than the water vapor temperature, so the water vapor is condensed. Condensate droplets (distilled water) appear and slide down following the inner glass surface and are received by the gutter and forwarded out (container).

2.2. Preparation of the absorbent charcoal briquettes

The solar heat absorber used in this study is an absorber plate painted black at the base of the basin and charcoal [37], in the form of additional briquettes of 3 types of wood. Charcoal briquettes of 3 types of wood are Kusambi wood (Schleichera oleosa), gama (Gliricidia sepium), and Kapok (Ceiba pentandra) obtained from the surrounding area, whose availability is relatively abundant. Furthermore, the names of the wood species above were converted into code form, namely SO_60 for charcoal briquettes of Kusambi wood (Schleichera oleosa), GS_60 for charcoal briquettes of Gamal wood (Gliricidia sepium) and CP_60 for charcoal briquettes of Kapok wood (Ceiba pentandra).

Figure 2. The process of making charcoal sorbents

The primary material for making charcoal is dry logs from three rich species that are found abundantly in the neighborhood. To make the charcoal, the dried logs were cut into 20-30 cm pieces and placed in three charcoal activation containers of the same size for height hours. After that, the charcoal was ground using a grinding machine and sieved using a shaker sieve to obtain a charcoal powder with a size of 60 mesh.

To make charcoal briquettes, the ground charcoal powder, tapioca flour, and hot water at a temperature of 100ºC were mixed. The percentage of the briquette mixture is 1% hot water, 1% tapioca flour, and 7% charcoal powder. After mixing and stirring evenly, the mixture was poured into a cylindrical mold and pressed using a pressing tool until it reached a briquette size 9 cm in diameter and 3 cm thick. The molded charcoal briquettes were then dried in the open air for three days with an average ambient temperature of 31ºC. After the charcoal briquettes were formed, they became a medium for absorbing and storing solar radiation heat for pre-treatment.

2.3. Experimental setup

The tests were carried out at the Laboratory of the Department of Mechanical Engineering, Faculty of Science and Engineering, Nusa Cendana University with a position of 10°09'13.7 "S south latitude 123°40'08.0 "E east longitude, on 22 July 2023-26 July 2023. Geographically coastal areas, lowlands, and hills with altitudes between 0-350 meters above sea level, with rates of temperatures between 29-34^{O}C and 71-90% of relative humidity. This study uses four basins that show four additional absorbent independent variables, namely CP_60, GS_60, SO_60 charcoal briquettes, and without charcoal briquettes (control).

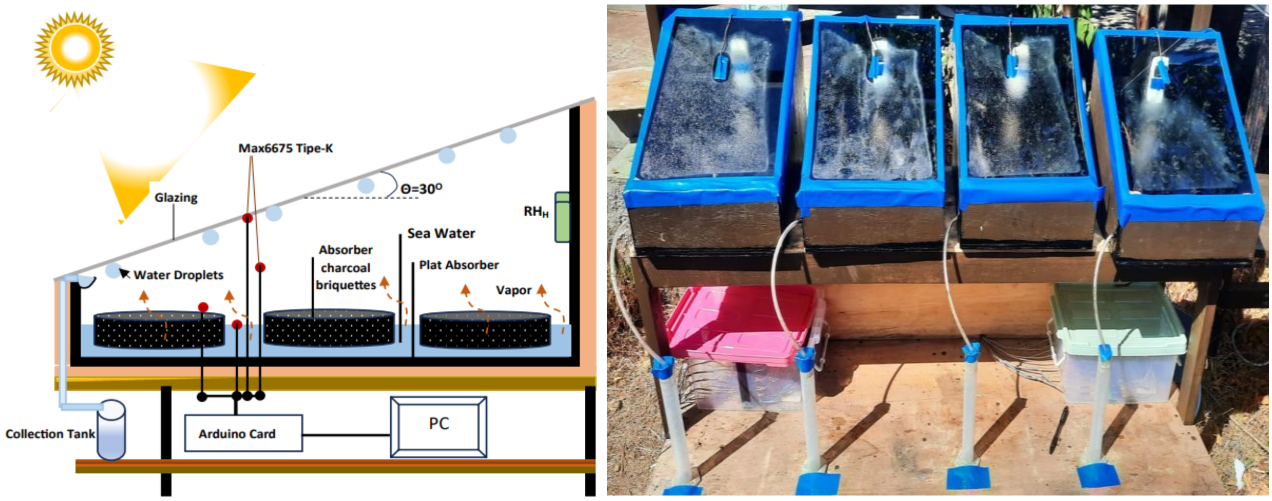

Figure 3. Experiment set up

The four basins were placed in an open space side by side facing north, not shadowing each other to allow maximum exposure to solar radiation. Measure the salt content of the seawater before filling each basin using a salinity meter and filling each basin with the same volume of 2 liters of seawater and placing charcoal (absorbent) briquettes for each desalination basin with the same size and number of briquettes. Placing temperature measuring instruments, namely AT4208 Multi-Chanel Temperature Data Logger 3.5 Inch and Max6675 Type-K thermocouple at the point of the charcoal briquette surface, seawater surface, basin space near the cover glass, cover glass, and the environment. Furthermore, it is connected to an electronic card called Arduino Mega [38]. The electronic card is connected to a PC via a USB cable, as shown in Figure 3. They placed Elitech RC-4HC temperature and humidity data loggers in each basin and room and placed a solar radiation intensity measuring instrument (Solar Power Meter SM206). Covering the basins with glass and ensuring there is no leakage of air and water vapor into or from the basins. Place a measuring cup outside the basin, connected to a pipeline from inside the basin, to measure the amount of water produced at any time. Recording test data with an interval of one hour in real time starting at 08:00 am to 04:00 pm for 8 hours following previous research [39].

3. Results and discussion

3.1. Test result

During the test, the intensity of solar radiation, ambient temperature, and humidity in each basin were measured and recorded in two graphs, Figures 1a and 1b. Figure 1 illustrates that the solar radiation intensity reached its peak at noon with a value of 1400.8 W/m2 and then decreased gradually until the end of the test period at 4:00 pm. The changes in solar radiation intensity affected the ambient temperature, as shown in the same graph. The ambient temperature initially increased and reached a maximum of 35^{O}C at 2:30 pm, then decreased until the end of the test time.

Figure 4b shows the variability of humidity in each desalination basin during the test. Relative humidity is the ratio between the water vapor content in the basin space and the maximum water vapor content that air can hold. At dew point temperature, RH is 100% which results in condensation. The water vapor content also depends on the water vapor pressure, which increases as the temperature rises due to the higher velocity of water vapor molecules.

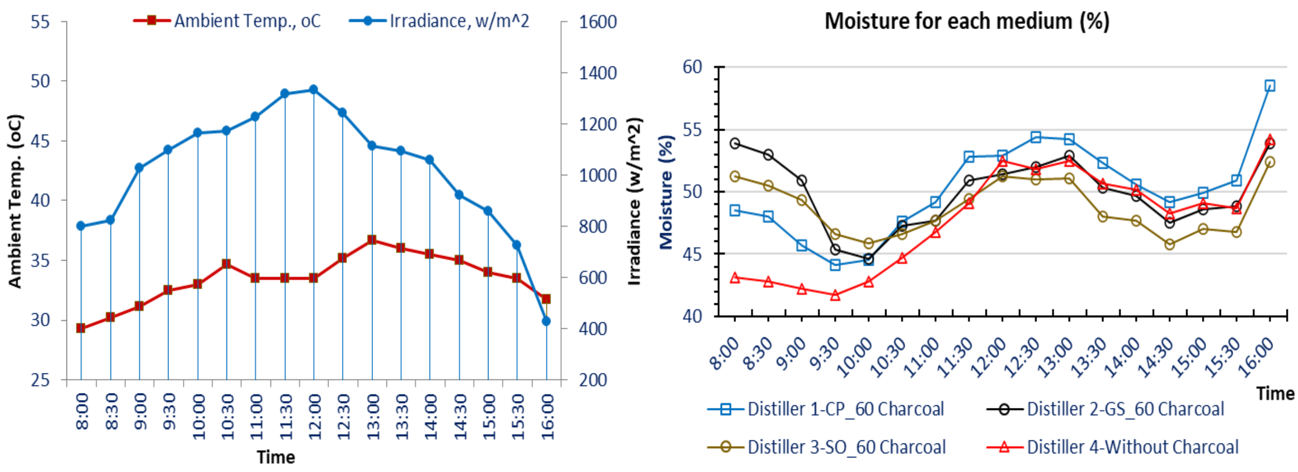

(a) (b)

Figure 4. (a) Variations in solar radiation and ambient temperature, (b) moisture variation in the basin

The humidity of each basin at the beginning of the test at 08:00 was relatively high and then decreased until 09:30. Then from 09:30 to 12:30 it increased, which then decreased again until 14:30.

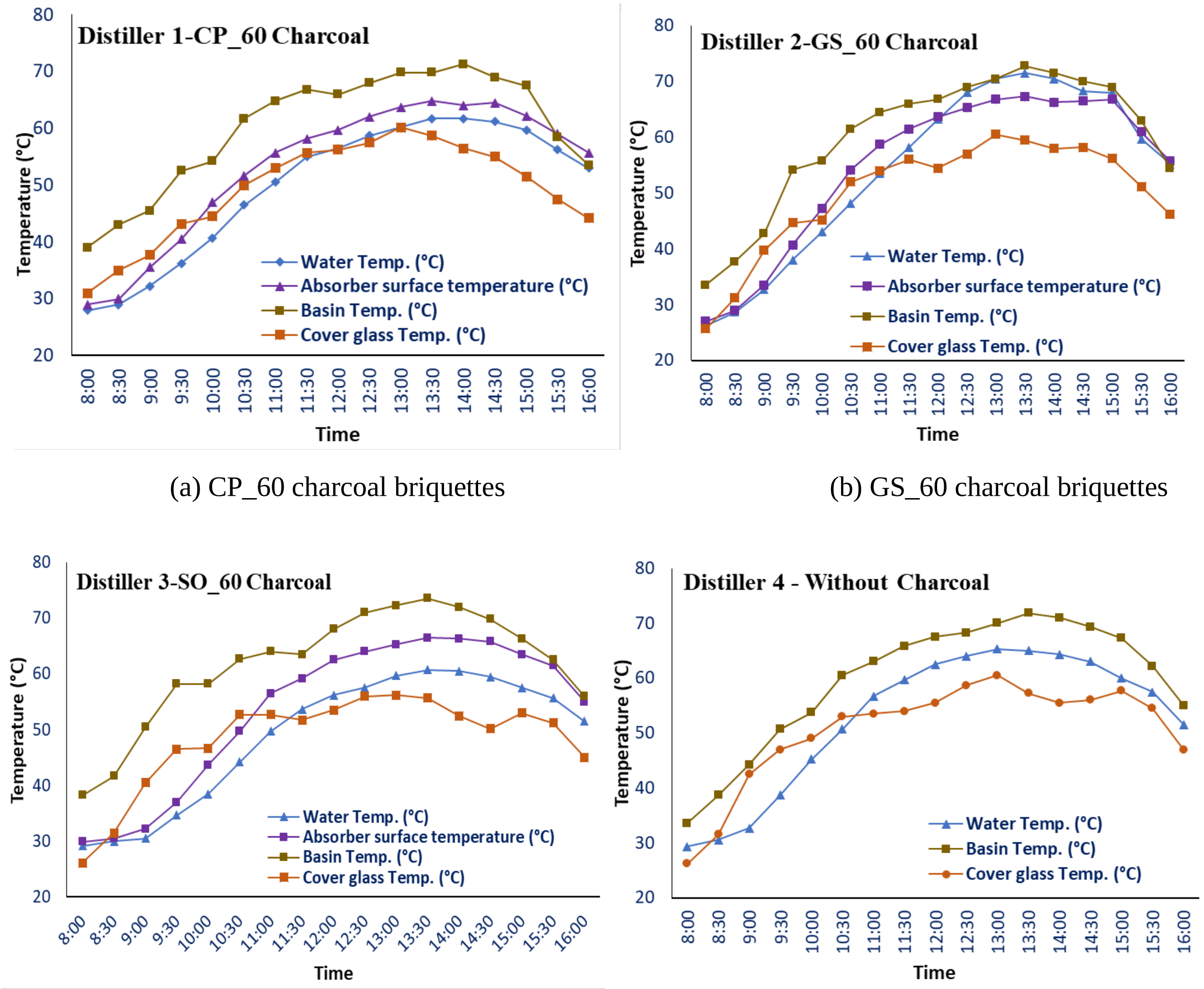

(a) CP_60 charcoal briquettes

(b) GS_60 charcoal briquettes

(c) SO_60 charcoal briquettes

(d) without charcoal briquettes

Figure 5. Temperature fluctuation vs retrieval time for test media relationship graph

During the test, the humidity levels fluctuated, with a notable increase from 15:00 until the end of the data collection at 16:00. When evaluating the results, it was observed that the SO_60 charcoal briquettes exhibited the lowest humidity, followed by the basin without charcoal briquettes, GS_60 charcoal briquettes, and finally the basin utilizing CP_60 charcoal briquettes, which displayed the highest humidity.

Figure 5 displays the temperature readings taken from the designated test points in each desalination basin. The results indicate that the temperature fluctuations for the 4 types of basins are nearly identical. During the testing period from 8:00 am to 4:00 pm, the temperature increased significantly from the start to the middle and then decreased gradually towards the end. Additionally, as shown in Figures 5a to 5d and 4a, the temperature patterns for all four basins and test points correlate with the solar radiation variation, consistent with previous research [40]. Figures 4a to 4d reveal that the lowest temperature point during data collection is at the cover glass, crucial for an optimal water vapor condensation process. The highest temperatures occur at the surface area of the charcoal briquettes (additional absorber), followed by the sea surface area and the basin space. The temperature fluctuations in the basin room are influenced by latent heat, specifically, the heat released during the evaporation process and condensation on the inner glass surface.

The graph displayed in Figure 6a showcases the distilled water production every 30 minutes for four desalination basins. The time frame for this observation is from 8:00 AM to 2:00 PM. It is important to note that each basin varies in the maximum amount of distilled water produced, and the time taken to produce it differs as well.

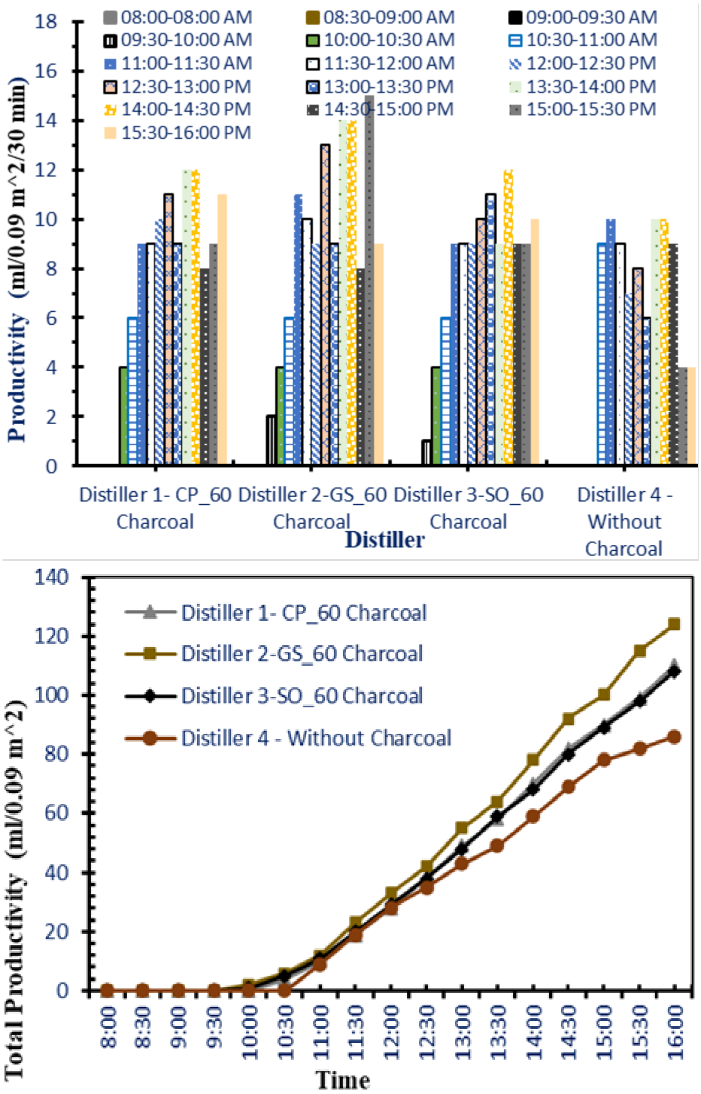

Figure 6. (a) Distillate water variation every 30 minutes (b) cumulative distillate water over the test time

For instance, the CP_60 charcoal briquettes produced a maximum of 12 ml of distilled water, which occurred between 1:30 PM to 2:00 PM. On the other hand, the GS_60 charcoal briquettes produced a maximum of 14 ml of distilled water, which occurred between 1:30 PM to 2:00 PM. Moreover, for the SO_60 charcoal briquettes, the maximum amount of distilled water produced was 11 ml, and it occurred between 1:00 PM to 1:00 PM. Lastly, the basin without charcoal briquettes produced a maximum of 10 ml of distilled water, which occurred between 1:30 PM to 2:00 PM.

Despite the differences in the maximum amount and time, all the basins showcase a similar trend. The production of distilled water increases from morning to noon and then decreases until 4:00 PM. This trend is in line with the decline in solar radiation, which affects the distillation process.

Figure 6b displays a cumulative graph that shows the total amount of distillate water for each desalination basin. The graph demonstrates that the GS_60 charcoal briquette test media provides the maximum total distillate water every 30 minutes. This also indicates that the Gamal wood charcoal briquettes have a better capacity to absorb and store heat compared to CP_60, SO_60, and the control (no charcoal briquettes).

The water temperature in each basin tends to be the same, but the distillate produced differs. The addition of different charcoal in each basin causes this condition. Charcoal is more effective at absorbing solar thermal energy than water [41][42]. The addition of charcoal will also affect the distillate water produced [43].

This happens because charcoal can store thermal energy for the solar desalination process, thus increasing its efficiency [44]. The difference in charcoal types lies in the porosity of each charcoal. This porosity affects the absorption of sunlight, and the wider the porosity of the charcoal, the higher the evaporation efficiency [45]. From the statistical test, the significance value of the effect of charcoal type on the desalination process was obtained. In this graph, the R-square value shows a significant effect due to the use of charcoal in the desalination process.

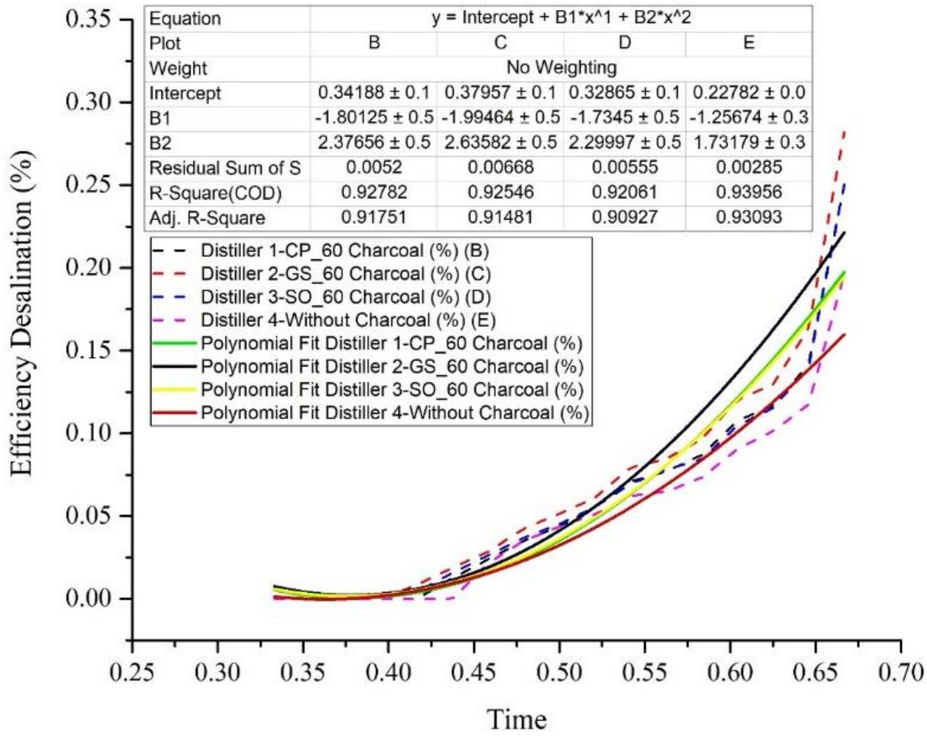

Figure 7. Statistical test of the effect of using charcoal-type

The study suggests that the use of natural absorbents, such as Gamal wood, can have a significant impact on the pace of evaporation, the effectiveness of desalination, and the overall volume of distilled water produced. By utilizing readily accessible and sustainable materials like Gamal wood, we can create a more environmentally friendly and cost-effective desalination system. This can increase the availability of clean water in rural areas or for people with restricted access to fresh water. The findings of this study have the potential to make it possible to apply more affordable and eco-friendly desalination technology in underserved locations.

There are some limitations and potential sources of error in this research. Different charcoal briquette properties can vary based on their composition, porosity, and surface area, which ultimately impact their absorption capabilities. To ensure consistent results, it is important to strictly standardize and characterize the briquettes used. Although this study tested three natural material-based auxiliary sorbents, it is important to note that numerous other materials with potential sorbent properties have yet to be explored. As a result, the findings may not apply to other types of sorbents.

3.2. Data analysis

The data analysis conducted in this test determines the use of an additional absorber to increase the evaporation rate, total distillate production, and desalination efficiency. The evaporation rate is a parameter that regulates distillate output. Meanwhile, efficiency is used to evaluate the performance of the system. The value of the evaporation rate was preceded by analyzing the convection heat transfer coefficient, the saturated vapor pressure at the water surface, and the vapor pressure at the glass surface. The convection heat transfer coefficient, h_{cwg}, between the water and glass surfaces for solar desalination is calculated by the equation developed by [46];

$$h_{cwg} = 0.884\left[\left(T_w - T_{gi}\right) + \frac{\left(P_w - P_{gi}\right)}{\left(2016 - P_w\right)}\right]^{1/3} \tag{1}$$

Description: hcwg = convection heat transfer coefficient (W/m2K), Pw = vapor pressure at the water surface (kPa), Pgi = vapor pressure inside glass surface (kPa), Tw = water surface temperature (°C), Tgi = inside glass surface temperature (°C).

To analyze the saturated vapor pressure at the water surface and glass surface, it can be calculated mathematically with the following equation [47];

$$P_w = 100\left(0.004516 + 0.0007178\,T_w - 2.6469 \times 10^{-6}\,{T_w}^2 + 6.944 \times 10^{-7}{T_w}^3\right) \tag{2}$$

$$P_{gi} = 100\left(0.004516 + 0.0007178\,T_{gi} - 2.6469 \times 10^{-6}\,{T_{gi}}^2 + 6.944 \times 10^{-7}{T_{gi}}^3\right) \tag{3}$$

Next, we can analyze the rate of evaporation, the equation used is the equation developed by [46];

$$h_{ewg} = \frac{9.15 \times 10^{-7} h_{cwg}\left(P_w - P_{gi}\right)h_{fg}}{\left(T_w - T_{gi}\right)} \tag{4}$$

hewg = evaporative heat transfer coefficient (W/m^{2}K), hfg = enthalpy of vapourization (kJ/kg).

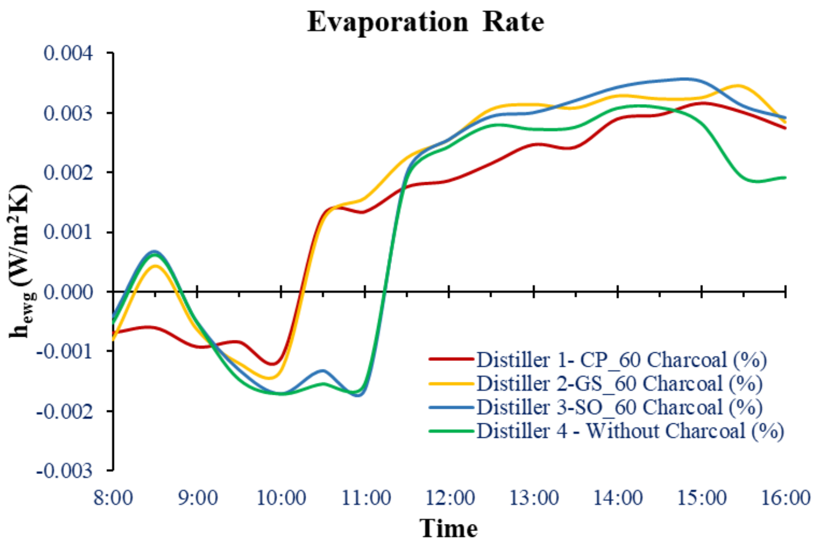

Figure 7. An hourly graph of the evaporative heat transfer coefficient for four basins

Convection heat transfer in the basin space is a heat transfer process followed by molecular movement of seawater due to heat received from solar radiation. When seawater is heated, thermal expansion occurs, which causes the mass density of seawater molecules to become light (buoyant). Thus, molecules that have a denser density will be replaced by lighter molecules. This process occurs continuously as the temperature rises; the molecules tend to move randomly and collide and begin to move quickly until some water molecules escape from the seawater layer and change form/phase to vapor. After evaporating, the vapor molecules move towards the cover glass. This process is called evaporation. The rate of evaporation in the basin is influenced by solar radiation, temperature, and humidity, as well as the characteristics of the seawater itself, namely volume and salinity.

Figure 7 shows the coefficient value of the evaporation rate of the basin using a natural additional absorber in the form of Gamal wood charcoal briquettes, which is the highest until 14:00, then decreases due to a decrease in solar intensity. The evaporation rate of the basin using the Gamal wood charcoal briquette auxiliary absorber reached its maximum value, followed by the basin using the Kusambi wood charcoal briquette auxiliary absorber, the basin using the Kapok wood charcoal briquette auxiliary absorber, and the lowest was the basin without the charcoal briquette auxiliary absorber. This data shows that charcoal briquettes increase the evaporation rate of seawater, but this process is still dependent on solar intensity.

Desalination efficiency is the ratio of the total latent heat of distillate evaporation to the solar energy entering the system [48]. It can be mathematically expressed as follows:

$$\eta_d = \frac{m_d \times h_{fg}}{A \times I_s} \times 100\% \quad (5)$$

ηd = efficiency of desalination (%), md = distillate production (kg/hour), hfg = enthalpy of vapourisation (kJ/kg), A = cross-sectional area of solar radiation receiver (m^2) dan Is = intensity of the sun (kJ/m^2.hour).

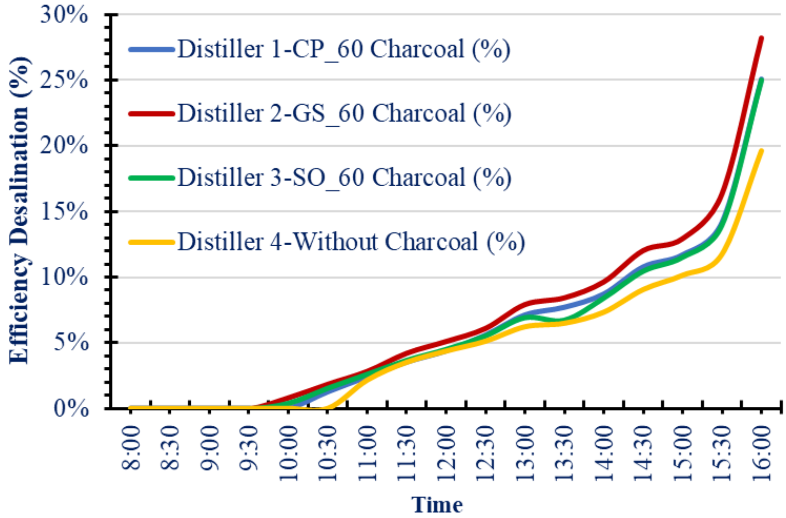

Figure 8. Desalination efficiency comparison chart for 4 basins every 30 minutes

The graph in Figure 8 shows the efficiency of each basin, namely, using the additional absorber of CP_60 charcoal briquettes, GS_60 charcoal briquettes, SO_60 charcoal briquettes, and without briquettes (control). Overall, the highest efficiency was shown by GS_60 charcoal briquettes, followed by CP_60 charcoal briquettes, SO_60 charcoal briquettes, and finally the control. The high mass flow rate of distillate water produced strongly influences the high efficiency of GS_60 charcoal briquettes. At 15.00 - 16.00, each basin shows a graphical pattern that increases significantly due to a decrease in solar intensity, which impacts decreasing temperature. This temperature is also inversely proportional to RH, where RH tends to increase (Figure 1). With the decrease in temperature and increase in RH, the result is that at that time, the water vapor molecules can reach their dew point faster and change to a liquid phase.

4. Conclusion

According to this research, the use of natural-based auxiliary sorbents, such as briquette charcoal, can have a significant impact on the efficiency of the desalination process. The study revealed that the GS_60 briquette charcoal type, in particular, can improve the performance of the desalination process by providing higher distillation yields and efficiency rates compared to other types of briquette charcoal. These findings suggest that using briquette charcoal, especially Gliricidia sepium, can enhance the efficiency and availability of clean water through desalination systems.

In order to enhance distillation efficiency and yield, future research aims to broaden the scope of sorbent types and characteristics beyond briquette charcoal. The objective is to gain a comprehensive understanding of other materials that possess the potential to serve as effective sorbents. Additionally, the research will delve deeper into analyzing the correlation between various environmental variables, including the porosity of briquette charcoal and evaporation efficiency.

Declaration of competing interest

The authors declare that they have no known financial or non-financial competing interests in any material discussed in this paper.

Funding information

This research was funded by the Directorate of Research, Technology, and Community Service through the 2023 National Competitive Research Program for State University Operational Assistance.

Acknowledgments

This research was funded by the Directorate of Research, Technology, and Community Service through the 2023 National Competitive Research Program for State University Operational Assistance.

Author contribution

The contribution to the paper is as follows: Muhamad Jafri, Ben Vasco Tarigan, Dominggus Godlief Heryson Adoe: study conception and design; Ben Vasco Tarigan, Dominggus Godlief Heryson Adoe: data collection; Muhamad Jafri, Ben Vasco Tarigan: analysis and interpretation of results; Muhamad Jafri, Ben Vasco Tarigan, Dominggus Godlief Heryson Adoe: draft preparation. All authors approved the final version of the manuscript.

References

[1] E. S. Ali, A. M. Farid, A. A. Askalany, M. Ghazy, A. E. Zohir, and A. S. Alsaman, ‘Cost analysis and performance investigation of solar-powered desalination system utilizing modified sodium polyacrylate adsorbent material’, *Energy Conversion and Management: X*, vol. 20, Oct. 2023, doi: 10.1016/j.ecmx.2023.100421.

[2] A. Hoque, A. H. Abir, and K. Paul Shourov, ‘Solar still for saline water desalination for low-income coastal areas’, *Appl Water Sci*, vol. 9, no. 4, Jun. 2019, doi: 10.1007/s13201-019-0986-9.

[3] Technology Association, ‘Water Desalination Processes’, American Membrane.

[4] K. K. Murugavel, Kn. K. S. K. Chockalingam, and K. Srithar, ‘Progresses in improving the effectiveness of the single basin passive solar still’, *Desalination*, vol. 220, no. 1–3, pp. 677–686, Mar. 2008.

[5] J. Bundschuh, M. Kaczmarczyk, N. Ghaffour, and B. Tomaszewska, ‘State-of-the-art of renewable energy sources used in water desalination: Present and future prospects’, *Desalination*, vol. 508. Elsevier B.V., Jul. 15, 2021. doi: 10.1016/j.desal.2021.115035.

[6] S. M. Asaad, A. Inayat, F. Jamil, C. Ghenai, and A. Shanableh, ‘Optimization of Biodiesel Production from Waste Cooking Oil Using a Green Catalyst Prepared from Glass Waste and Animal Bones’, *Energies (Basel)*, vol. 16, no. 5, Mar. 2023, doi: 10.3390/en16052322.

[7] A. M. Makarieva, V. G. Gorshkov, and B.-L. Li, ‘Energy budget of the biosphere and civilization: Rethinking environmental security of global renewable and non-renewable resources’, *Ecological Complexity*, vol. 5, no. 4, pp. 281–288, Dec. 2008.

[8] Z. Said and A. Mehmood, ‘Standalone photovoltaic system assessment for major cities of United Arab Emirates based on simulated results’, *J Clean Prod*, vol. 142, no. 4, pp. 2722–2729, Jan. 2017.

[9] S. Shoeibi, M. Saemian, S. M. Parsa, M. Khiadani, S. A. A. Mirjalily, and H. Kargarsharifabad, ‘A novel solar desalination system equipped with thermoelectric generator, reflectors and low-cost sensible energy-storage for co-production of power and drinking water’, *Desalination*, vol. 567, p. 116955, Dec. 2023.

[10] A. Kumar, A. K. Tiwari, and Z. Said, ‘A comprehensive review analysis on advances of evacuated tube solar collector using nanofluids and PCM’, *Sustainable Energy Technologies and Assessments*, vol. 47, Oct. 2021, doi: 10.1016/j.seta.2021.101417.

[11] K. Sampathkumar and P. Senthilkumar, 'Utilization of solar water heater in a single basin solar still—An experimental study', *Desalination*, vol. 297, pp. 8–19, Jul. 2012.

[12] T. Arunkumar, R. Jayaprakash, A. Ahsan, D. Denkenberger, and M. S. Okundamiya, 'Effect of water and air flow on concentric tubular solar water desalting system', *Appl Energy*, vol. 103, pp. 109–115, 2013, doi: 10.1016/j.apenergy.2012.09.014.

[13] N. Rahbar, J. A. Esfahani, and A. Asadi, 'An experimental investigation on productivity and performance of a new improved design portable asymmetrical solar still utilizing thermoelectric modules', *Energy Convers Manag*, vol. 118, pp. 55–62, Jun. 2016.

[14] K. Srithar, T. Rajaseenivasan, N. Karthik, M. Periyannan, and M. Gowtham, 'Stand alone triple basin solar desalination system with cover cooling and parabolic dish concentrator', *Renew Energy*, vol. 90, pp. 157–165, May 2016.

[15] H. Tanaka and Y. Nakatake, 'A simple and highly productive solar still: a vertical multiple-effect diffusion-type solar still coupled with a flat-plate mirror', *Desalination*, vol. 220, no. 3, pp. 287–300, Mar. 2005.

[16] A. Sohani, S. Hoseinzadeh, and K. Berenjkar, 'Experimental analysis of innovative designs for solar still desalination technologies; An in-depth technical and economic assessment', *J Energy Storage*, vol. 33, p. 101862, Jan. 2021.

[17] S. Shoeibi and H. Kargarsharifabad, 'Effects of nano-enhanced phase change material and nano-coated on the performance of solar stills', *J Energy Storage*, vol. 42, p. 103061, Oct. 2021.

[18] A. I. Shehata *et al.*, 'Enhancement of the productivity for single solar still with ultrasonic humidifier combined with evacuated solar collector: An experimental study', *Energy Convers Manag*, vol. 208, p. 112592, Mar. 2020.

[19] P. Khalilmoghadam, A. R. Ghahnavieh, and M. B. Shafii, 'A novel energy storage system for latent heat recovery in solar still using phase change material and pulsating heat pipe', *Renew Energy*, vol. 163, pp. 2115–2127, Jan. 2021.

[20] S. M. Parsa, A. Rahbar, M. H. Koleini, S. Aberoumand, M. Afrand, and M. Amidpour, 'A renewable energy-driven thermoelectric-utilized solar still with external condenser loaded by silver/nanofluid for simultaneously water disinfection and desalination', *Desalination*, vol. 480, p. 114354, Apr. 2020.

[21] D. G. H. Samuel, P. K. Nagarajan, R. Sathyamurthy, S. A. El Agouz, and E. Kannan, 'Improving the yield of fresh water in conventional solar still using low cost energy storage material', *Energy Convers Manag*, vol. 112, pp. 125–134, Mar. 2016.

[22] S. Shanmugan, S. Palani, and B. Janarthanan, 'Productivity enhancement of solar still by PCM and Nanoparticles miscellaneous basin absorbing materials', *Desalination*, pp. 186–198, May 2018, doi: 10.1016/j.desal.2017.11.045.

[23] M. M. Naima, M. A. Abd, and E. Kawib, 'Non-conventional solar stills Part 1. Non-conventional solar stills with charcoal particles as absorber medium', *Desalination*, vol. 153, pp. 55–64, 2002, [Online]. Available: www.elsevier.com/locate/desal

[24] A. S. Nafey, M. Abdelkader, A. Abdelmotalip, and A. A. Mabrouk, 'Solar still productivity enhancement', *Energy Convers Manag*, vol. 42, no. 11, pp. 1410–1408, Jul. 2001.

[25] T. V. Arjunan, H. S. Aybar, and Orfi. Jamel, 'Performance Analysis of Solar Desalination Systems', in *Solar Desalination Technology*, 2019, pp. 75–104.

[26] S. Abdallah, M. M. Abu-Khader, and O. Badran, 'Effect of various absorbing materials on the thermal performance of solar stills', *Desalination*, vol. 242, no. 1–3, pp. 128–137, Jun. 2009.

[27] T. Elango, A. Kannan, and K. K. Murugavel, 'Performance study on single basin single slope solar still with different water nanofluids', *Desalination*, vol. 360, pp. 45–51, Mar. 2015.

[28] C. E. Okeke, ~ S U Egarievwe, and A. 0 E. Anmalu, 'NOTE EFFECT'S OF COAL AND CHARCOAL ON SOLAR-STILL PERFORMANCE', 1990.

[29] J. T. Mahdi, B. E. Smith, and A. O. Sharif, 'An experimental wick-type solar still system: Design and construction', *Desalination*, vol. 267, no. 2–3, pp. 233–238, Feb. 2011, doi: 10.1016/j.desal.2010.09.032.

[30] A. Sharma, V. V. Tyagi, C. R. Chen, and D. Buddhi, 'Review on thermal energy storage with phase change materials and applications', *Renewable and Sustainable Energy Reviews*, vol. 13, no. 2. pp. 318–345, Feb. 2009. doi: 10.1016/j.rser.2007.10.005.

[31] C. E. Okeke, ~ S U Egarievwe, and A. 0 E. Anmalu, 'EFFECT'S OF COAL AND CHARCOAL ON SOLAR-STILL PERFORMANCE', *Energi*, vol. 15, no. 11, pp. 1071–1073, 1990.

[32] A. Sadoun, A. Khechekhouche, I. Kemerchou, M. Ghodbane, and B. Souyei, 'Impact of natural charcoal blocks on the solar still output', *Heritage and Sustainable Development*, vol. 4, no. 1, pp. 61–66, Apr. 2022, doi: 10.37868/hsd.v4i1.80.

[33] A. Khechekhouche, B. Benhaoua, M. Manokar, R. Sathyamurthy, A. E. Kabeel, and Z. Driss, 'Sand dunes effect on the productivity of a single slope solar distiller', *Heat and Mass Transfer/Waerme- und Stoffuebertragung*, vol. 56, no. 4, pp. 1117–1126, Apr. 2020, doi: 10.1007/s00231-019-02786-9.

[34] H. Panchal, 'Performance Investigation on Variations of Glass Cover Thickness on Solar Still: Experimental and Theoretical Analysis', *Technology and Economics of Smart Grids and Sustainable Energy*, vol. 1, no. 1, Dec. 2016, doi: 10.1007/s40866-016-0007-0.

[35] A. Khechekhouche, A. M. Manokar, R. Sathyamurthy, F. A. Essa, M. Sadeghzadeh, and A. Issakhov, 'Energy, Exergy Analysis, and Optimizations of Collector Cover Thickness of a Solar Still in El Oued Climate, Algeria', *International Journal of Photoenergy*, vol. 2021, 2021, doi: 10.1155/2021/6668325.

[36] R. Cherraye, B. Bouchekima, D. Bechki, H. Bouguettaia, and A. Khechekhouche, 'The effect of tilt angle on solar still productivity at different seasons in arid conditions (south Algeria)', *International Journal of Ambient Energy*, vol. 43, no. 1, pp. 1847–1853, 2022, doi: 10.1080/01430750.2020.1723689.

[37] A. Sadoun, A. Khechekhouche, I. Kemerchou, M. Ghodbane, and B. Souyei, 'Impact of natural charcoal blocks on the solar still output', *Heritage and Sustainable Development*, vol. 4, no. 1, pp. 61–66, Apr. 2022, doi: 10.37868/hsd.v4i1.80.

[38] Learn Arduino, 'Arduino - Temperature Sensor (tutorialspoint.com)', Learn Arduino. Accessed: Oct. 02, 2023. [Online]. Available: https://www.tutorialspoint.com/arduino/arduino_temperature_sensor.htm

[39] A. Hoque, A. H. Abir, and K. Paul Shourov, 'Solar still for saline water desalination for low-income coastal areas', *Appl Water Sci*, vol. 9, no. 4, Jun. 2019, doi: 10.1007/s13201-019-0986-9.

[40] A. E. Kabeel, Z. M. Omara, F. A. Essa, A. S. Abdullah, T. Arunkumar, and R. Sathyamurthy, 'Augmentation of a solar still distillate yield via absorber plate coated with black nanoparticles', *Alexandria Engineering Journal*, vol. 56, no. 4, pp. 433–438, Dec. 2017, doi: 10.1016/j.aej.2017.08.014.

[41] C. E. Okeke, ~ S U Egarievwe, and A. 0 E. Anmalu, 'NOTE EFFECT'S OF COAL AND CHARCOAL ON SOLAR-STILL PERFORMANCE', 1990.

[42] S. Temmar, A. Khelef, M. H. Sellami, R. Cherraye, A. Khechekhouche, and S. E. Laouini, 'Effect of different carbon types on a traditional solar still outp', *Desalination Water Treat*, vol. 284, pp. 11–18, Feb. 2023, doi: 10.5004/dwt.2023.29292.

[43] Benarima Zine El Abidine, L. Abdelhamid, M. H. Sellami, and B. Hamza, 'Experimental Study to Improve the Solar Desalination Performance Using Local Heat Storage Material', *Journal of Water Chemistry and Technology*, vol. 45, no. 2, pp. 154–163, Apr. 2023, doi: 10.3103/s1063455x2302011x.

[44] J. Roslan, W. E. Kan, A. K. Abdul Rahman, M. Suliman, and R. Isha, ‘Charcoal characterization and application is solar evaporator for seawater desalination’, in *IOP Conference Series: Materials Science and Engineering*, Institute of Physics Publishing, Mar. 2020. doi: 10.1088/1757-899X/736/2/022107.

[45] H. Abdelrazeq and M. Khraisheh, ‘Porosity Effect of Polystyrene Membranes on Desalination Performance: A Combined Experimental and Numerical Heat and Mass Transfer Study in Direct Contact Membrane Distillation’, *Polymers (Basel)*, vol. 15, no. 8, Apr. 2023, doi: 10.3390/polym15081821.

[46] V. Belessiotis, S. Kalogirou, and E. Delyannis, *Thermal Solar Desalination*. Chennai, India: Academic Press, 2016.

[47] S. A. Kalogirou, *Solar Energy Engineering Processes and Systems*, 2nd ed. Amsterdam: Elsavier, 2014.

[48] H. Zheng, *Solar Energy Desalination Technology*. Beijing: Elsevier, 2017.